Czech Pattern Recognition Workshop 2000, Tomáš Svoboda (Ed.)
Peršlák, Czech Republic, February 2–4, 2000
Czech Pattern Recognition Society

Adaptive 3D Acquisition using Laser Light

Christian Liska
Austrian Research Centers Seibersdorf
Authorised Javacenter
Breitenfurter Strasse 43-45, A-1120 Vienna
christian.liska@ajc.at

Robert Sablatnig
Vienna University of Technology
Pattern Recognition and Image Processing Group
Favoritenstrasse 9/183-2, A-1040 Vienna
sab@prip.tuwien.ac.at

Abstract

In order to reconstruct the viewable surface of an object completely, multiple views of the same object have to be used and integrated into a common coordinate system. One of the major problems of the 3d surface reconstruction using a turntable, is the varying resolution in the direction to the camera, due to the varying distance of object points to the rotational axis of the turntable. To guarantee a uniform object resolution, we calculate the next angle dynamically, depending on the entropy of the surface part actually acquired. To minimize the loss of information and to guarantee a uniform surface resolution, we derive a relation between the entropy and the next viewing angle, based on the profile sections acquired in the last two steps of the acquisition.

1 Introduction

The reconstruction of the viewable object surface requires images from multiple views. The number of acquisition steps and the respective orientation of the camera relative to the object surface are unknown for arbitrary objects [4, 13]. Therefore, we need techniques, which estimate the next sensor position based on the measurement of the shape information captured in previous steps of the acquisition process and therefore generating a relationship between the sensor and the object of interest [12].

In this paper, we present a next-view-planning technique which estimates the next sensor position depending on the object's surface structure. The system relies only on the data acquired, where the position of the first acquisition step is arbitrary. Then, the next positions are estimated based on the profile section acquired in the previous step of the process. Following an initial image acquisition, prominent features such as surface and shape characteristics are extracted and used for a subsequent registration of the actual view with the 3d-data acquired so far. Next, the newly acquired data is used to decide where the next sensor position should be, in order to scan the surface optimally. Depending on the already performed acquisition steps, a decision is made whether it is necessary to make further acquisition steps or not.

The paper is organized as follows: Section 2 describes the acquisition system and its geometric arrangement. Section 3 describes the strategy for estimating the next sensor position based on the surface structure and Section 4 presents experimental results showing the balance between surface resolution and amount of data. Finally, in Section 5 conclusions are drawn and future work is outlined.

2 Acquisition System

The acquisition method used for estimating the 3d-shape of objects is shape from structured light, based on active triangulation [1]. The camera is positioned between the two lasers facing the measurement area. The complete system consists of:

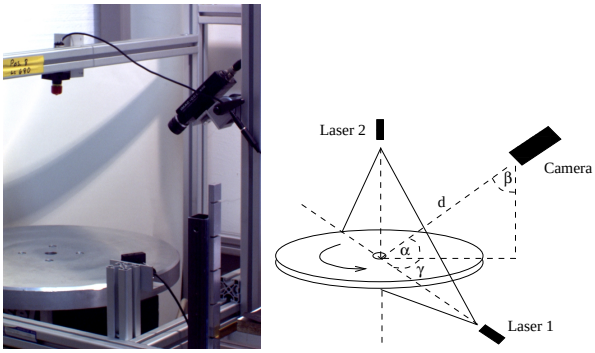

(a) Equipment (b) Arrangement

Figure 1: Acquisition system.

1. 1 turntable with a diameter of 50 cm, which can be rotated about the z-axis, used to move the object of interest through the acquisition area.

2. 2 red lasers to illuminate the scene, one mounted on the top (distance to rotation plane is 45 cm), one beside the turntable (distance to the rotation center is 48 cm). Both lasers are extended with cylindrical lenses to spread the laser beam into one illuminating plane. The laser light

plane intersects with the object surface, forming one laser stripe.

3. 1 CCD-camera (b/w) with a 16 mm focal length, a resolution of 768x572 pixels, and a distance of 40 cm to the rotation center. The angle between the camera normal vector and the rotation plane is approx. 45 degrees. A frame grabber card is used to connect the camera to a PC.

4. 1 Intel Pentium PC under Linux operating system.

Figure 1 depicts the complete hardware setup (a) and its geometric arrangement (b).
There are several reasons to use two lasers instead of one. One of the most important reason is occlusion. Two kinds of occlusions appear in the field of 3d surface reconstruction:

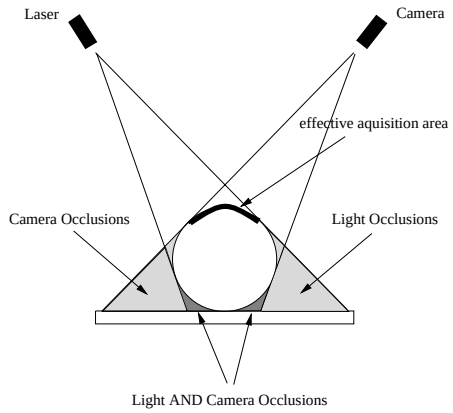

Figure 2: Light and camera occlusions.

1. Light occlusions: A ray of light cannot reach the complete surface.

2. Camera occlusions: Parts of the surface are invisible to the camera.

Light and camera occlusions are shown in Figure 2, the effective acquisition area (shown in bold) where light and camera "see" the surface is relatively small in comparison to the viewing angle of the camera. The reduction of light occlusions by adding a second laser is shown in Figure 3. The turntable reduces the camera occlusions, since the object is acquired in different directions.

To accomplish the calibration of the system we need three steps:

1. Camera calibration: To get the intrinsic and extrinsic parameters of the camera we use Tsai's method [15]. The results are encoded in a 3x4-DLT-Matrix, as shown in [10].

2. Turntable calibration: We compute the orientation of the rotational plane and the 3d position of the center of revolution. Due to the nature of the multi plane calibration approach of [15], the calibration of the turntable is done simultaneously with the camera calibration [14].

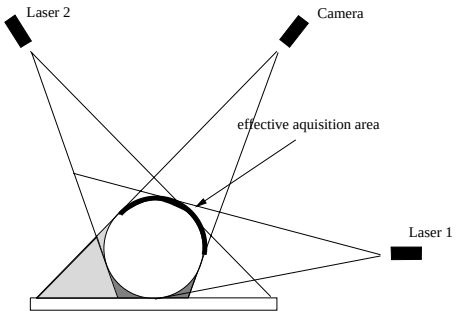

Figure 3: Reduction of light occlusions.

3. Laser plane calibration: The orientation of the laser light plane is determined by a multi plane approach [2].

The extrinsic parameters (orientation) of the camera, the parameters of the rotational plane, the center of revolution and the laser plane are represented in the same reference coordinate system.

3 Sensor Planning

The problem of 3d-acquisition using a turntable is the varying resolution in direction to the camera due to the varying rotation of object points in respect to the rotational axis of the turntable [6, 7]. Therefore, we use a next view planning technique [4] that ensures an optimal (in the sense of information content and amount of data) object surface resolution and makes it possible to sense high-structured parts of the object in higher resolution than parts with uniform structure. Since the class of objects to be scanned has no predictable shape and orientation, no predetermined sampling pattern can guarantee that all of the visible surfaces of an object will be scanned [9]. An adaptive scanning pattern derived by next view planning reduces the amount of unscanned areas. In contrast to model-based approaches like [16], where a general purpose model used to characterize a scene or environment is validated actively with statistical methods, our approach is focused on handling occlusions.

The problem solutions on estimating the next best view (NBV) can be divided into three categories:

- Minimization of occlusions: Occlusions are interpreted as filled polygons. Then, a set of sensor positions and angles relative to the object's surface are computed for each pixel of these polygons. The result of this step is a set of intervals from which the polygon pixel is visible. Decomposing these intervals gives the next sensor position. Whereas [4, 3] analyses range images, [8] uses volume models, to solve the NBV-Problem.

- Analyzing the geometric properties of the surface: In [5] the surface structure is given by triangulated surface points. The surface is completed by stepwise refinement. Regions, which show highly structured parts will be scanned with higher density than regions which show low structured parts.

- Heuristic search and objective functions: The set of next sensor positions is reduced by applying a heuristic search. The best position is estimated by maximizing an objective function [11, 17].

The result of the first category approaches is information about the position and orientation of occlusions in the scene. This information is two or three dimensional. To reduce occlusions, a system, which allows a movement of more than one degree of freedom is needed. The turntable allows a movement about the z-axis and the next best sensor position will be estimated by the analysis of the surface structure. The notion of the next "best" sensor position can be defined in two ways:

- The system should achieve a minimal number of acquisition positions and steps to reconstruct the object of interest.

- Computing those acquisition positions and directions, which gives the best reconstruction results.

In this work, we develop a system, which achieves a minimal number of acquisition steps by accomplishing given accuracy requirements.

3.1 Adaptive Image Acquisition

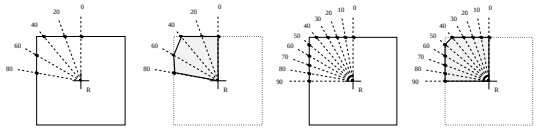

(a) 20 degrees (b) 10 degrees

Figure 4: Sampling with equiangular steps.

One of the major problems of the 3d surface reconstruction using a turntable, is the varying resolution in the direction to the camera, due to the varying distance of object points to the rotational axis of the turntable. The varying resolution leads to a loss of surface features. Figure 4 shows two examples to the loss of information. Sampling the object with a constant angle of 20 degrees (Figure 4a), we loose one corner of the square. On the other side, sampling the object with a lower constant angle, the loss of information is less (Figure 4b) than sampling with a higher constant angle. Therefore, the accuracy of reconstructions can be improved by decreasing the sampling angle, whereas the effort of the acquisition process will be increased.

3.2 Complexity

The maximum number of acquisition steps depends on the camera resolution. Therefore the minimum angle is given by

$$\phi_{min} = \arctan \frac{r}{A}, \tag{1}$$

where r is the distance of one surface point to its center of revolution and A is the resolution of the camera. The maximum number of acquisition steps is then given by

$$N_{max} = \frac{360}{\phi_{min}}. \tag{2}$$

Let n be the desired number of maximal acquisition steps. The complexity of the NBV-problem is then given by

$$C_{NBV} = \sum_{i=1}^{n} \binom{N_{max}}{i}, \tag{3}$$

viewed as the more general set theory problem of finding a minimal number of subsets that completely covers a set [13], which is in the class of NP complete problems and therefore only solvable with polynomial effort.

The limitation to a directed movement and the definition of a maximum angle ϕ_{max} reduces the complexity, because the number of possible next positions will be decreased.

3.3 Computing the Next Sensor Position

To estimate the next sensor position, we have to calculate the distance of the captured surface points relative to the axis of rotation. The calculation of the next rotational angle is given by the following expressions:

- Defining and calculating a distance function: Let L be a set of back transformed surface points P given by one acquisition step. For each of these points, we calculate the Euclidean distance d_{norm} to its axis of rotation $R_{axis} = R + v \cdot S$, where S is the direction of the axis of rotation. d_{norm} is given by

$$d_{norm} = \frac{|S \times (P - R)|}{|S|}. \tag{4}$$

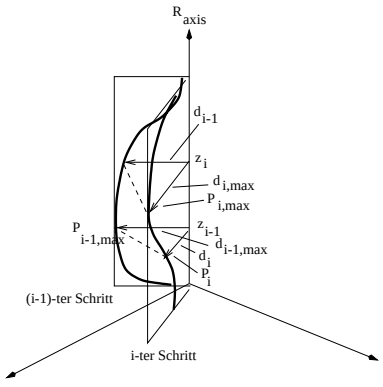

Figure 5: Calculating the next viewing angle.

- Defining and calculating the gradient of one surface point: Be $P_{i,max}$ the surface point with the maximum Euclidean distance d_{norm} to R_{axis} in the i-th acquisition step. The information content or *entropy* of the surface point is

defined as the absolute gradient of d_{norm} in point P: $g_i = d'_{norm}(P)$, calculated by the following algorithm (see also Figure 5):

1. Estimation of $d_{i,max}$: This is explicitly given by $P_{i,max}$ (see Figure 6).

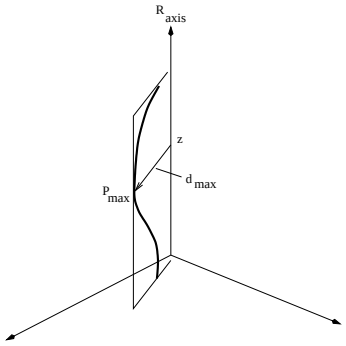

Figure 6: Calculating the normal distance.

2. Estimation of the surface point P_{i-1} (acquired in the previous step $i-1$) with the same z-component as $P_{i,max}$ and calculation of $d_{i-1}(P_{i-1})$.
3. Computation of the approximated gradient g_a between d_{i-1} and $d_{i,max}$. Since d is not known completely during the acquisition process, the first derivative of d' is not computable. Therefore, g_a is approximated by the gradient of the line between P_i and P_{i-1}:

$$g_i = \frac{d(P_i) - d(P_{i-1})}{\phi(P_i) - \phi(P_{i-1})}, \tag{5}$$

where $\phi(P)$ denotes the absolute rotation angle of P (see Figure 7).

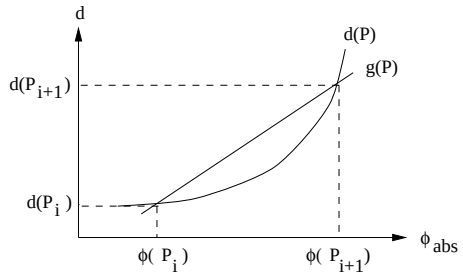

Figure 7: Approximated gradient of distance function d

4. Computation of the gradients angle α_a of g_a: $alpha_a = \arctan g_a$.
5. Estimation of the surface point P_i with the same z-component as the point $P_{i-1,max}$ and calculation of $d_i(P_i)$.
6. Computation of the approximated gradient g_b between $d_{i-1,max}$ and d_i.
7. Computation of the gradients angle α_b of g_b.
8. Estimation of the region with the highest entropy. This region is denoted by $max(\alpha_a, \alpha_b)$.

- Calculation of the next rotation angle: The gradient value could be positive, negative or zero, depending on an increasing, decreasing or unchanging entropy (i.e. g_i). Table 1 shows the calculation of the relative change $\phi_{i,rel}$ and the absolute angle $\phi_{i,abs}$ depending on the sign of the gradient g_i, the gradient angle α_i and the relative change $\phi_{i-1,rel}$ of the $(i-1)$-th step. The parameter ϕ_{min} denotes the minimal rotation angle, ϕ_{max} the maximal rotation angle, and the threshold t_α encodes the geometric conditions under which the system sampling density will be increased (see [2] for details).

ent. g_i	grad. α_i	prev. angle $\phi_{i-1,rel}$	next angle $\phi_{i,rel}$	abs. angle $\phi_{i,abs}$
> 0	$> t_\alpha$	$> \phi_{min} \cdot 2$	$\frac{\phi(P_i)-\phi(P_{i-1})}{2}$	$\phi_{i-1} - \phi_{i,rel}$
		$< \phi_{min} \cdot 2$	ϕ_{min}	$\phi_{i-1} - \phi_{i,rel}$
		$= \phi_{min}$	ϕ_{min}	$\phi_{i-1} + \phi_{i,rel}$
> 0	$\leq t_\alpha$	$-$	$\phi_{i-1,rel}$	$\phi_{i-1} + \phi_{i,rel}$
< 0	$> t_\alpha$	$> \phi_{min} \cdot 2$	$\frac{\phi(P_i)-\phi(P_{i-1})}{2}$	$\phi_{i-1} - \phi_{i,rel}$
		$< \phi_{min} \cdot 2$	ϕ_{min}	$\phi_{i-1} - \phi_{i,rel}$
		$= \phi_{min} \cdot 2$	ϕ_{min}	$\phi_{i-1} + \phi_{i,rel}$
< 0	$\leq t_\alpha$	$< \phi_{max}/2$	$\phi_{i-1,rel} \cdot 2$	$\phi_{i-1} + \phi_{i,rel}$
		$\geq \phi_{max}/2$	ϕ_{max}	$\phi_{i-1} + \phi_{i,rel}$
$= 0$	$= 0$	$< \phi_{max}/2$	$\phi_{i-1,rel} \cdot 2$	$\phi_{i-1} + \phi_{i,rel}$
		$\geq \phi_{max}/2$	ϕ_{max}	$\phi_{i-1} + \phi_{i,rel}$

Table 1: Next rotation angle.

Table 1 shows that the next rotation angle depends on the entropy, the gradient angle and the previous rotation angle. If for instance the entropy increases and the previous rotation angle is high, a negative absolute rotation angle ensures that the higher structured area is scanned again. If the entropy decreases, the absolute rotation angle is increased.

3.4 Surface Reconstruction

An iterative process for 3d surface reconstruction in static environments is defined by the following steps (see also Figure 8, which depicts this process):

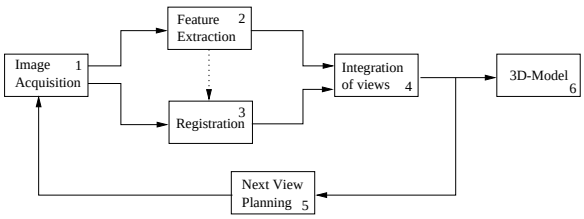

Figure 8: Iterative procedure for 3d surface reconstruction.

1. Image acquisition: The scene is captured by the CCD-camera. The result is a greyscale- image which shows the intersection between the laser plane and the object which is a line (left image in Figure 9).

2. Feature extraction: The line shown in the camera image is extracted. The result is a set of 2d points (middle image in Figure 9 shows a graphical representation of such a set).

3. Registration: The set of 2d points extracted in the previous step is transformed from the world coordinate system in its object coordinates. The right image in Figure 9 shows a graphical representation of back projected points extracted at the previous step.

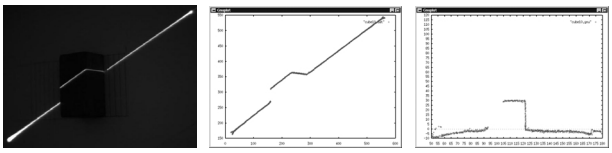

Figure 9: Acquisition, extraction and backprojection of an intersection line.

4. Integration: Each registered point is integrated into the existing model computed and integrated at the previous iterations of the acquisition process. Figure 10 shows the reconstruction and visualization of a cube after six iterations.

5. Next View Planning: The next viewing angle is computed based on the algorithm shown in the previous section and the turntable moves to the calculated absolute angle. The process repeats until the turntable revolves one complete rotation.

6. 3d-model visualization of the reconstructed surface.

4 Results

Figure 11 shows the reconstruction of an archaeological amphore. The symmetry axis of the pottery and the rotational axis of the turntable are roughly justified. The minimum angle was defined as $\phi_{min} = 4deg$ and the maximum angle as $\phi_{max} = 12deg$. Analyzing the reconstructed data shows a displacement of 1.8 mm in x-direction and 2.1 mm in y-direction. Therefore, the object was sampled with varying relative angles in 36 steps.

The next object of interest is a cube with a side length of 3 cm. Figure 1 shows the partial reconstruction after an absolute angle of 90 degrees. The minimum angle was defined

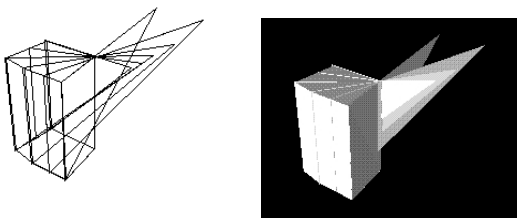

Figure 10: Integration and visualization.

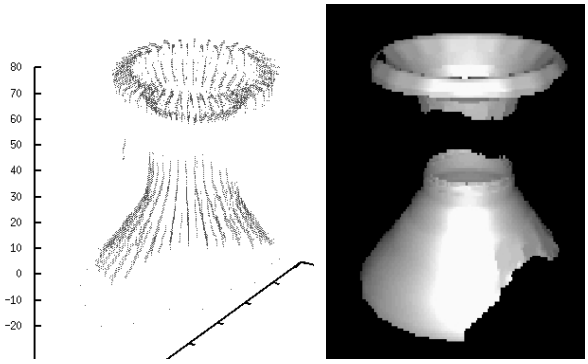

(a) reconstr. (b) rendered

Figure 11: Reconstruction of arch. pottery.

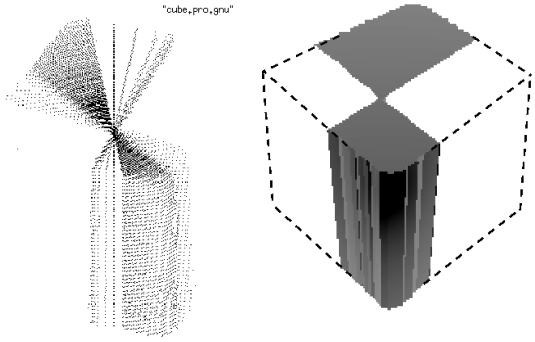

(a) reconstr. (b) rendered

Figure 12: Partial reconstruction of a cube.

with $\phi_{min} = 1deg$, the maximum angle as $\phi_{max} = 8deg$. Because of the higher entropy of this region, we see a higher sampling density at the cube's corner. The acquisition needs 50 steps.

Sampling	Steps	Percent of 90
1 degree equiangular	90	100
8 degree equiangular	11	12
NVP - adaptive	50	55

Table 2: Cube sampling.

Table 2 shows the balance between sampling with equiangular and adaptive steps. 90 steps would be necessary to scan the object in full resolution, if the resolution is decreased to 8 degrees equiangular, the detail at the corner is lost. Using the NVP approach the detail at the corner is kept whereas the number of acquisition steps is decreased by 55%.

5 Summary and Future Work

We have presented a next-view-planning technique to reduce the computational effort in 3d surface reconstruction using a turntable up to 50% without decreasing the quality of reconstruction. The surface resolution (measured in terms of information content or entropy with respect to the distance of the rotational axis of the turntable) is preserved since the gradient between surface points is used to determine the sampling rate and thus the next sensor position.

Future work will be directed towards increasing the DoF of the acquisition system in the z-direction to minimize camera occlusions. This will help to increase the variety of different shapes that can be scanned with constant surface resolution. Currently the entropy is computed out of two profiles only. By increasing the number of profiles taken to determine the next rotation angle highly structured objects can be scanned more accurately. Furthermore, the use of simple volume models will allow a real time visualization.

6 Acknowledgements

This work was supported in part by the Austrian Science Foundation (FWF) under grant P13385-INF.

References

[1] F. DePiero and M.Trivedi. *3-D computer vision using structured light: Design, calibration, and implementation issues*. Advances in Computers, 1996.

[2] C. Liska. Das adaptive Lichtschnittverfahren zur Oberflächenrekonstruktion mittels Laserlicht. Technical Report PRIP-TR-055, PRIP, TU Wien, 1999.

[3] J. Maver. Necessary views for a coarse representation of a scene. In *Proc. of 13th. Intl. Conf. on Pattern Recognition, Vienna, Austria*, pages 936–940, 1996.

[4] J. Maver and R. Bajcsy. Occlusions as a guide for planning the next view. *IEEE Trans. on Pattern Analysis and Machine Intelligence*, 15(5):417–432, May 1993.

[5] M. Milroy, C. Bradley, and G. Vickers. Automated laser scanning based on orthogonal cross sections. *Machine Vision and Applications*, 9:106–119, 1996.

[6] W. Niem. Error analysis for silhouette-based 3D shape estimation from multiple views. In N. Sarris and M. Strintzis, editors, *Proc. of Intl. Workshop on Synthetic-Natural Hybrid Coding and Three-Dimensional Imaging*, pages 143–146, 1997.

[7] W. Niem. Automatic reconstruction of 3d objects using a mobile camera. *Image and Vision Computing*, 17(2):125–134, February 1999.

[8] D. Papadopoulos-Orfanos and F. Schmitt. Automatic 3-D digitization using a laser rangefinder with a small field of view. In *Proceedings of the Intl. Conf. on Recent Advances in 3-D Digital Imaging and Modeling*, pages 60–67, Ottawa, Canada, May 1997.

[9] R. Pito. A solution to the next best view problem for automated surface acquisition. *IEEE Trans. on Pattern Analysis and Machine Intelligence*, 21(10):1016–1030, October 1999.

[10] W. Pölzleitner and M. Ulm. Robust camera calibration for spacecraft motion estimation. In *Image Analysis and Synthesis, Schriftenreihe der österreichischen Computergesellschaft, Bd. 68*, pages 115–136, 1993.

[11] V. Sequeira, J. G. M. Gonçalves, and M. I. Ribeiro. Active view selection for efficient 3D scene reconstruction. In *Proc. of 13th. Intl. Conf. on Pattern Recognition, Vienna, Austria*, pages 815–819, 1996.

[12] K. A. Tabanis, P. K. Allan, and R. Y. Tsai. A survey of sensor planning in computer vision. *IEEE Transactions on Robotics and Automation*, 11(1):86–104, February 1995.

[13] G. H. Tarbox. Planning for complete sensor coverage in inspection. *Computer Vision and Image Understanding*, 61(1):84–111, January 1995.

[14] S. Tosovic. Lineare Hough-Transformation und Drehtellerkalibrierung. Technical Report PRIP-TR-059, PRIP, TU Wien, 1999.

[15] R. Y. Tsai. An efficient and accurate camera calibration technique for 3D machine vision. pages 364–374, Miami Beach, FL, 1986.

[16] P. Whaite and F. Ferrie. On the sequential determination of model misfit. *IEEE Trans. on Pattern Analysis and Machine Intelligence*, 19(8):899–905, August 1997.

[17] H. Zha, K. Morooka, T. Hasegawa, and T. Nagata. Active modeling of 3-D objects: Planning on the next best pose (NBP) for acquiring range images. In *Proceedings of the Intl. Conf. on Recent Advances in 3-D Digital Imaging and Modeling*, pages 68–75, Ottawa, Canada, May 1997.